

1 Novel keto-alkyl-pyridinium antifungal molecules active in models of in vivo *Candida albicans*
2 vascular catheter infection and ex vivo *Candida auris* skin colonization.

3

4 Running title: Novel pyridinium antifungal molecule

5

6 Sarah R. Beattie¹, Taiwo Esan², Robert Zarnowski^{3,4}, Emily Eix^{3,4}, Jeniel E. Nett^{3,4}, David R.

7 Andes^{3,4}, Timothy Hagen², Damian J. Krysan^{1, 5, 6}

8

9 Department of Pediatrics, Department of Pediatrics, Carver College of Medicine, University of
10 Iowa, Iowa City IA¹; Department of Chemistry and Biochemistry, Northern Illinois University,
11 1425 West Lincoln Highway, DeKalb IL²; Department of Medicine, Section of Infectious Disease,
12 University of Wisconsin, Madison WI³; Department of Medical Microbiology and Immunology,
13 University of Wisconsin, Madison WI⁴; Department of Microbiology/Immunology, Carver College
14 of Medicine, University of Iowa, Iowa City IA⁵; Department of Molecular Physiology and
15 Biophysics, Carver College of Medicine, University of Iowa, Iowa City IA⁶.

16

17

18

19 Corresponding Author:

20 Damian J. Krysan

21 2040 Med Labs 25 S. Grand Avenue, Department of Pediatrics, Microbiology/Immunology, and
22 Molecular Physiology and Biophysics, Carver College of Medicine, University of Iowa, Iowa City
23 Iowa 52242, Phone: 319-335-3066, damian-krysan@uiowa.edu

24

25

26

27 **Abstract**

28 New antifungal therapies are needed for both systemic, invasive infections as well as superficial
29 infections of mucosal and skin surfaces as well as biofilms associated with medical devices. The
30 resistance of biofilm and biofilm-like growth phases of fungi contributes to the poor efficacy of
31 systemic therapies to non-systemic infections. Here, we describe the identification and
32 characterization of a novel keto-alkyl-pyridinium scaffold with broad spectrum activity (2-16
33 µg/mL) against medically important yeasts and moulds, including clinical isolates resistant to
34 azoles and/or echinocandins. Furthermore, these keto-alkyl-pyridinium agents retain substantial
35 activity against biofilm phase yeast and have direct activity against hyphal *A. fumigatus*.
36 Although their toxicity precludes use in systemic infections, we found that the keto-alkyl-
37 pyridinium molecules reduce *C. albicans* fungal burden in a rat model of vascular catheter
38 infection and reduce *Candida auris* colonization in a porcine ex vivo model. These initial pre-
39 clinical data suggest that molecules of this class may warrant further study and development.

40

41

42

43

44

45

46

47

48

49

50

51

52

53 Introduction

54 The effective treatment of human fungal infections is reliant on a relatively small set of
55 structurally and mechanistically distinct drugs: azoles, polyenes, and echinocandin/triterpenoid
56 glucan synthase inhibitors (1). As has been extensively discussed in the literature, this limited
57 antifungal pharmacopeia must be expanded to meet the challenging clinical needs of patients in
58 the 21st century (2). Two specific examples where current antifungal therapies are relatively
59 ineffective are: 1) infections involving biofilm on medical devices and mucosal surfaces (3) and
60 2) decolonization of *Candida auris* from skin (4). As with antibacterial agents, fungal biofilms are
61 highly resistant to the currently used antifungal drugs (3). Consequently, removal of *Candida*
62 infected medical devices such as vascular catheters and prosthetic joints is the standard of care
63 (5), whereas devices infected with some species of bacteria are frequently salvaged with
64 antibiotic therapy alone (6).

65 *C. auris* is an emerging fungal pathogen with many unusual characteristics compared to
66 other *Candida* species (3). For example, it is readily transmitted from one patient to another in
67 the hospital setting (7). This is very uncommon for other fungal pathogens and is likely due to its
68 ability to persistently colonize patient's skin as well as the inanimate surfaces in hospitals and
69 long-term care facilities. Standard biocides used to decolonize microbes (e.g., methicillin-
70 resistant *Staphylococcus aureus*) from patient's skin such as chlorhexidine have relatively poor
71 activity against *C. auris* (8). Furthermore, *C. auris* is frequently resistant to at least one of the
72 three major classes of antifungal drugs (9) and pan-resistant isolates have been reported with
73 increasing frequency (10). As such, *C. auris* is a pernicious problem that can result in
74 therapeutically intractable infections.

75 One approach to treating surface-associated fungal infections such as biofilms and skin
76 colonization is to identify molecules that are mechanistically distinct from those used to treat
77 systemic infections and are specifically developed for that purpose. Such molecules could be
78 imagined to display the general properties of traditional antiseptics but with activity optimized for

79 specific organisms or improved safety profile. Here, we describe a set of novel N-keto alkyl
80 pyridinium ions with broad spectrum antifungal activity against both planktonic and biofilm phase
81 fungi.

82 Pyridinium-based anti-septic/anti-infective molecules have been studied and developed
83 for topical and, in some instances, possible systemic use. Molecules in this class have been
84 explored for antifungal applications (11, 12). For example, the long chain N-alkylated pyridinium
85 cetylpyridinium chloride, a component of commercial mouthwashes, has in vitro activity against
86 *Candida* spp with minimum inhibitory concentrations (MIC) of 2-6 µg/mL in modified CLSI
87 conditions (13). A recent repurposing screen found that the anti-parasitic pyridinium-class drug
88 pyrvinium pamoate is active against *C. auris* (MIC 2 µg/mL, ref. 14). Bis(pyridinium) molecules
89 with variously sized alkyl or aryl linkers have also been shown to have antifungal activity (11,
90 15). One study showed that the bis(pyridinium) compounds induced less red blood cell lysis
91 than similar bis(quaternary-ammonium) compounds (15).

92 The series characterized in this report are mono-pyridinium ions with aryl-alkyl ketone
93 substituents at the N atom of the pyridinium ring (Fig. 1A). The molecules are comparable in
94 activity to the commercially used, cetylpyridinium chloride and pyrvinium pamoate and have
95 activity in an in vivo rat model of *C. albicans* vascular catheter infection as well as in an ex vivo
96 model of *C. auris* skin colonization.

97

98 **Results**

99 **Aryl methyl keto-N-alkylated pyridinium molecules have broad spectrum antifungal**
100 **activity.**

101 A set of small molecule libraries were screened for compounds against *Aspergillus*
102 *fumigatus* using recently developed high throughput screening assay applicable for this
103 filamentous mould (16). A molecule with the aryl methyl keto-N-alkylated pyridinium (**keto-alkyl**
104 **pyridinium**, KAP) scaffold (Fig. 1A) was identified a hit in the screen. A set of analogs of this

105 initial hit were prepared and tested, leading to two derivatives with similar activity profiles
106 (compounds **A** and **B**, Fig. 1A); **C** was used a control as it is inactive but has a very similar
107 chemical structure compared to the active derivatives. Although >30 KAP derivatives were
108 prepared, no clear structure-activity relationships (SAR) could be identified to explain the
109 variation in antifungal properties of this series (see Fig. S1 for general synthesis approach).
110 Pyridinium cations are widely believed to target membranes as part of their mechanism of action
111 and a non-protein target could explain this difficult-to-interpret SAR (13, 17). Although other
112 potential targets have also been proposed, a biochemically or genetically confirmed alternative
113 target to the membrane has not been reported (12, 14). It is, however, interesting that small
114 changes in substitution patterns in comparing A/B to C (Fig. 1A) lead to dramatic changes in
115 antifungal activity without clearly identifiable changes in physicochemical properties. These
116 observations suggest that the molecules have structurally specific interactions with a target and
117 imply that interaction with membranes is not solely due to their amphipathic properties.

118 The scope of the antifungal activity for compounds A and B was explored by CLSI
119 methods for a range of fungal pathogens including yeasts and moulds (Table 1). In general, A/B
120 are more consistently active against yeasts compared to moulds (*A. fumigatus*, *A. terreus*, and
121 *F. oxysporum*). Although the MIC for some isolates of *A. fumigatus* was similar to those for
122 yeast, significant strain-to-strain variability in activity toward *Aspergillus* was observed. We also
123 tested A/B against two fluconazole-resistant *C. albicans* strains (TWO15/17, ref. 17) that have
124 increased expression of efflux pumps. We no difference in susceptibility compared to the
125 reference strain SC5314 (Table 1). Furthermore, compounds A and B were both active against
126 drug susceptible (0381) and multi-drug resistant (0390) *C. auris* isolates (Table 1).

127 Since pyridinium cations such as cetylpyridinium chloride also have activity against
128 bacteria, we tested compounds A and B against the Gram-positive bacteria, *Staphylococcus*
129 *aureus*, and the Gram-negative bacteria, *Pseudomonas aeruginosa*. Compared to
130 cetylpyridinium chloride, compounds A and B were ~32-fold less active against *S aureus* but

131 were more active against *P. aeruginosa* (32 µg/mL vs 250 µg/mL reported in ref 17). In
132 contrast, the activity of A/B were within 2-fold of the MICs reported for cetylpyridinium chloride
133 against *C. albicans* and pyrvinium pamoate against *C. auris*.

134 To determine if compound interacted with clinically used antifungal drugs, we performed
135 checkerboard assays and determined fractional inhibitory concentration indices. Compound B
136 showed additive interactions with both caspofungin and amphotericin B against *C. albicans* but
137 showed a complex interaction with fluconazole. The FICI for compound B and fluconazole is
138 8.25 due to the 8-fold increase in fluconazole concentration in the combination; however, the
139 concentration of compound B in at FIC is reduced by 4-fold relative to compound A as a single
140 agent. Interestingly, Edlind et al. also observed that cetylpyridinium chloride showed antagonism
141 with fluconazole and induced expression of the efflux pumps *CDR1* and *CDR2* (13).

142 In contrast to the antagonistic interaction of compound B with fluconazole in *C. albicans*,
143 voriconazole, the gold standard therapy for aspergillosis, showed an additive interaction.
144 Indeed, the activity of compound B was improved 8-fold in combination with voriconazole at ½
145 MIC. These data indicate that the induction of relative azole resistance in *C. albicans* by B does
146 not occur with *A. fumigatus*. Efflux pump mediated resistance to azoles is not as prevalent in *A.*
147 *fumigatus* compared to *C. albicans* and, thus, the mechanisms of efflux pump induction and
148 function are not as well defined.

149

150 **KAPs are active against *Candida* biofilms and *A. fumigatus* hyphae**

151 In general, pyridinium cations are too toxic for systemic administration because many
152 examples of this class directly lyse red blood cells (15). Consistent with those expectations,
153 compound A and B cause significant red blood cell lysis (LD₅₀ A: 26.9 µg/mL; B: 78.6 µg/mL;
154 and C > 1000 µg/mL, Fig. S1) while compound C, which has no antifungal activity also had no
155 activity against red blood cells. This observation provides implicit support for the membrane as
156 an important target of these molecules. Both A and B also showed toxicity against the human

157 cell line HegG2 with LD₅₀ of 9 µg/mL and 20 µg/mL using cell lysis and metabolic activity
158 assays, respectively (Fig. S1). Consequently, the KAPs, like other quaternary nitrogen anti-
159 infectives, are likely to be suitable for topical or other non-systemic applications and not feasible
160 for systemic therapy.

161 As discussed above, many anti-infectives have dramatically reduced activity against
162 biofilm phase organisms compared to the planktonic growth phase of standard CLSI activity
163 assays. To test the activity of the compounds against fungal biofilms, we generated a 24 hr
164 biofilm of *Candida albicans* and then treated with a dilution series of the compounds for an
165 additional 24 hr. The metabolic activity of the biofilms was then assayed using the standard XXT
166 reduction assay (19). Consistent with planktonic results, compound A was active (Fig. 2A, IC₅₀ =
167 18.4 µg/mL) while C was not. The biofilm activity of compound A was reduced by 4-fold relative
168 to planktonic growth (MIC 4 µg/mL, Table 1). Interestingly, the activity of compound A was
169 slightly higher against *C. auris* biofilms (Fig. 2B IC₅₀ = 5 µg/mL) relative to planktonic growth
170 (MIC 8 µg/mL, Table 1).

171 CLSI testing of antifungal activity of moulds is based on inoculation with conidia and,
172 therefore, measures inhibition of germination (20). For example, voriconazole is the gold
173 standard for treatment of pulmonary infection and inhibits germination. The most important *A.*
174 *fumigatus* infection that requires non-systemic therapy is fungal keratitis (21). At the time of
175 clinical presentation, *A. fumigatus* is exclusively in the hyphal form. We, therefore, were
176 interested to determine if compound A or B was active against *A. fumigatus* hyphae. *A.*
177 *fumigatus* CEA10 was incubated for 24 hr prior to exposure to a dilution series of compound B
178 or C for an additional 24 hr. The metabolic activity of the cultures was determined using
179 resazurin as previously described (17). The IC₅₀ (3.9 µg/mL, Fig. 2C) of compound B against
180 this strain was slightly lower than its MIC (8 µg/mL, Table 1) determined by CLSI methods. To
181 further characterize the mode of action of the KAPs against *A. fumigatus* hyphae, we treated
182 CEA10 with compound B for 24 hr and then stained the cells with propidium iodide, a dye that is

183 excluded from cells with intact membranes (Fig. 2D). Whereas cells treated with DMSO control
184 showed essentially no staining, B-treated cells showed uniform uptake of dye, indicating loss of
185 membrane integrity. Taken together, these data indicate that KAPs directly kill hyphal stage *A.*
186 *fumigatus*.

187

188 **KAP A is efficacious in an in vivo model of *C. albicans* venous catheter infection.**

189 One potential approach to managing central venous catheter infections is to treat the
190 lumen of the catheter with an anti-infective solution that is locked within the catheter and not
191 introduced into the patient (22). This strategy is most often applied to catheters infected with
192 bacteria but has been proposed for fungal infections as well (5, 6). To test the efficacy of KAPs
193 in this setting, a rat model of *C. albicans* venous catheter infection was employed (23). The
194 catheter was infected with *C. albicans* SC5314 and, on post-infection day 1, treated with A (8
195 $\mu\text{g}/\text{mL}$ solution within catheter) or vehicle. After 24 hr, the catheter was removed and processed
196 for fungal burden and scanning electron microscopy. Compound A-treated catheters showed >
197 1 \log_{10} reduction in fungal burden relative to vehicle-treated catheters (Fig. 3A). Consistent with
198 these results, the treated catheters showed dramatic in the extent of remaining biofilm. Thus,
199 compound A is able to disrupt a pre-formed *C. albicans* biofilm in vitro and in vivo.

200

201 **KAP A reduces *C. auris* colonization of skin in an ex vivo porcine model**

202 The ability of *C. auris* to colonize human skin is likely associated with its persistence in
203 infected patients and its ability to transmit from person-to-person (7). Because compound A
204 showed comparable activity against *C. auris* during planktonic and inanimate-substrate biofilm
205 growth, we tested its activity in an ex vivo porcine model of *C. auris* skin colonization (24).
206 Consistent with these in vitro data, compound A reduced the fungal burden of the colonized
207 porcine skin by $\sim 1 \log_{10}$ at a concentration of 8 $\mu\text{g}/\text{mL}$ (Fig. 4). The fungal burden was not
208 reduced further at 16 $\mu\text{g}/\text{mL}$ of compound A, suggesting that absorption/adsorption or

209 physicochemical factors may limit efficacy. The activity of compound A was greater than that of
210 2% chlorhexidine ($\sim 0.5 \log_{10}$ reduction, ref. 8) and comparable to the synergistic activity of 2%
211 chlorhexidine/70% isopropanol ($1.0 \log_{10}$ reduction, ref. 8). We note that, due to limitations in
212 compound A availability, that the data for skin treated with compound A was collected 24 hr
213 after a single treatment while the studies with chlorhexidine and 70% isopropanol were based
214 on a 72 hr experiment with three daily applications of study compounds. These experimental
215 distinctions notwithstanding, compound A shows promising activity against *C. auris* and is likely
216 at least as effective, and possibly more effective, than 2% chlorhexidine.

217

218 Discussion

219 Although new therapeutic options for systemic therapy of fungal infections are sorely
220 needed (2), agents with promise in the treatment of other types of fungal infections, particularly
221 those involving biofilm and biofilm-like growth phases, would also be quite valuable (3,4). Here,
222 we have characterized the activity of a structurally novel series of pyridinium cation-based
223 antifungal molecules and demonstrate their potential for the treatment of non-systemic fungal
224 infections. Compounds A and B show comparable or improved activity relative to other cationic
225 nitrogen-based anti-infectives/anti-septics such as chlorhexidine and cetylpyridinium chloride
226 against fungal pathogens (8, 13, 14). In addition, A and B have similar activity to the pyridinium-
227 based drug pyrvinium pamoate against *C. auris* against in vivo biofilms (14), further supporting
228 the utility of this class of molecule against this important emerging and drug-resistant pathogen.

229 Our in vivo and ex vivo experiments provide compelling proof-of-principle data for the
230 potential use of these scaffolds in the setting of antifungal lock therapy for intravascular
231 catheters and as possible disinfectants for *C. auris* skin colonization. With respect to the latter,
232 compound A is more active than the widely studied chlorhexidine (8) which was shown to have
233 activity in a mouse model of colonization (25). Since these compounds are variations on
234 previously validated chemical structures with application to topical and other non-systemic uses,

235 a strong premise exists for their potential development. Additional potential applications for
236 which our data provide support are oropharyngeal candidiasis and fungal keratitis. The latter
237 infection is a globally important cause of blindness for which there is no generally effective
238 medical therapy (21). Compounds A and B have reasonable activity against the two most
239 common etiologic agents of fungal keratitis: *A fumigatus* and *Fusarium* spp (Table 1). The direct
240 activity against hypha is an important feature of this series but additional optimization will be
241 needed to improve the consistency of activity and therapeutic index to become useful for fungal
242 keratitis.

243 The mechanism of action for quaternary nitrogen-based antifungals such as the KAPs is
244 likely to involve, at least in part, the direct disruption of membrane structures (17). Recent work
245 by Sim et al. suggested that pyrvinium pamoate interferes with mitochondrial function (14) and
246 mode of action studies of the cationic amidine antifungal candidate T-2307 as well as other
247 cationic ammonium antifungals also showed that mitochondrial disruption contributes to their
248 activity (12, 26). A hallmark of mitochondrial disruption in *C. albicans* is an inability to grow on
249 non-fermentable carbon sources such as glycerol. Indeed, the MIC of T-2307 decreases
250 dramatically when the cells are grown on 2% glycerol compared to 2% dextrose (26). We,
251 however, did not detect a change in MIC for compounds A or B when tested in the same
252 medium with glycerol instead of glucose as carbon source, indicating that mitochondrial
253 disruption is unlikely to be a major mode of action (data not shown). Attempts to generate
254 resistant mutants by serial passaging were also unsuccessful which further suggests either
255 multiple targets or non-protein targets such as the membrane are likely to contribute to the
256 antifungal activity of the KAPs.

257 It is interesting that compound A that, like cetylpyridinium chloride, is antagonistic with
258 fluconazole in *C. albicans* in checkerboard assays. Edlind et al. showed that cetylpyridinium
259 chloride induces the expression of the efflux pumps *CDR1* and *CDR2* but that deletion of these
260 genes has no effect on its activity (13). Compounds A and B are active as reference strains

261 against fluconazole-resistant clinical strains shown to have increased expression of efflux
262 pumps (Table 1, ref. 18). Thus, it seems that both types of pyridinium based antifungal
263 molecules alter expression of fluconazole pumps without being susceptible to their effects. As
264 such, these observations imply that they have similar mechanisms of action that are best
265 attributed to membrane disruption.

266 In summary, we provide in vitro and in vivo data suggesting that the KAP-type pyridinium
267 cation molecules may be promising new agents for the non-systemic treatment of fungal
268 infections.

269

270

271

272

273

274

275

276

277

278

279

280

281

282

283

284

285

286

287

288

289

290

291

292 **Materials and methods**

293 **Strains, media, reagents and instrumentation.** All yeast strains were maintained on YPD
294 from 25% glycerol stocks stored at -80°C. All *A. fumigatus* strains were maintained on glucose
295 minimal media (GMM; (33) from 25% glycerol stocks stored at -80°C. *A. fumigatus* CFF clinical
296 isolates were received from Dr. Robert Cramer (Dartmouth College), SPF98 was received from
297 Dr. W. Scott Moye-Rowley (University of Iowa), *C. neoformans* DUMC clinical isolate series
298 were received from Dr. John Perfect (Duke University). Reagents were purchased as at least
299 reagent grade from Aldrich, Acros or Alfa Aesar unless otherwise specified and used without
300 further purification. Solvents were purchased from Fischer Scientific (Pittsburgh, PA) and were
301 either used as purchased or redistilled with an appropriate drying agent. Compounds used for
302 structure–activity studies were synthesized according to methods described below, and all the
303 compounds were identified to be least 95% pure using HPLC. Analytical TLC was performed
304 using precoated Silica G TLC Plates, w/UV254, aluminum backed, purchased from Sorbtech
305 (Norcross, GA) and visualized using UV light. Flash chromatography was carried out using with
306 a Biotage Isolera One (Charlotte, NC) system using the specified solvent. Microwave reactions
307 were performed using Biotage Initiator+ (Charlotte, NC). Purity analysis were performed on an
308 Agilent 1100 HPLC utilizing a C-18 column (Waters Nova-Pak; 3.9 x 100 mm) with the following
309 method: Solvent A = H₂O (0.1% TFA), Solvent B = Acetonitrile; 0 to 20 min, (10 to 90% B), 20 to
310 25 min (90 to 10% B); detection was set at two wavelengths (245 and 280 nm). Purity of all final
311 compounds was above 95%. All final compounds were analyzed by high resolution MS

312 (HRMS) using a Bruker Maxis Plus Quadrupole Time-of-Flight (QTOF or QqTOF). ^1H and ^{13}C
313 NMR were recorded on either a BrukerAvance III 500 outfitted with a 5mm BBFO Z-gradient
314 probe or a Avance III 300 instrument is equipped with a 5 mm BBFO probe. The chemical shifts
315 are expressed in parts per million (ppm) using suitable deuterated NMR solvents.

316

317 **Dichlorodiphenylmethane (1).**

318 To a round flask was weighed benzophenone (1eq) and PCl_5 (1.5eq). The reaction was refluxed
319 for 2 h at 150°C . After 2 hours, the reaction was cooled, 40 mL of DCM was added to the
320 resultant solution followed by transferring to 250 mL Erlenmeyer flask. The resultant solution
321 was cooled to 0°C and 40 mL of distilled water was added. The resultant solution was
322 transferred to a separatory funnel, the DCM layer was separated, washed twice with 40 mL
323 distilled water, and dried with anhydrous sodium sulfate. The DCM solvent was evaporated in
324 rotary evaporator to give corresponding dichloride. The crude product was immediately used for
325 the next step without purification.

326

327 **2-chloro-1-(2,2-diphenylbenzo[d][1,3]dioxol-5-yl)ethenone (2)**

328 To a round flask was weighed dichlorodiphenylmethane (1 g, 4.2 mmol) and 2-chloro-1-(3, 4-
329 dihydroxyphenyl) ethanone (0.79 g, 4.2 mmol) under nitrogen. The reaction was refluxed at
330 180°C for 30mins under nitrogen. After 30 mins. The crude product was transferred to silica gel
331 chromatography with linear gradient of 2 - 10% (EtOAc/Hexane). The fractions corresponding to
332 the desired product were collected and solvent evaporated using rotatory evaporator to give
333 yellow viscous liquid as the desired product which turned to a solid upon dryness. Yield; 0.7 g,
334 47%, ^1H NMR (500 MHz, CDCl_3) δ 7.69 (m, 4H), 7.61-7.57 (m, 2H), 7.44 (m, 6H), 6.98 (d, J =
335 7.9 Hz, 1H), 4.63 (s, 2H). ^{13}C NMR (75 MHz, CDCl_3), 189.26, 152.05, 148.05, 139.46, 129.56,
336 129.01, 128.41, 125.14, 118.58, 108.52, 108.38, 45.84

337

338 **4-acetamido-1-(2-(2,2-diphenylbenzo[d][1,3]dioxol-5-yl)-2-oxoethyl)pyridin-1-ium chloride**

339 **(3)**. To a round flask containing 2-chloro-1-(2,2-diphenylbenzo[d][1,3]dioxol-5-yl)ethenone (0.34
340 0.97 mmol) dissolved in acetonitrile (10 mL) was weighed the 4-aminopyridine (0.09 g, 0.97
341 mmol). The reaction was refluxed for 2hrs at 100°C in which precipitate was formed. After 2 hrs,
342 the solvent was evaporated using rotatory evaporator and the gummy solid precipitated with
343 10% Hexane in DCM, filtered and dried to give a powdered solid product in form of the chloride
344 salt. HPLC purity; 98%. Yield; 0.38 g, 88%, ¹H NMR (300 MHz, DMSO) δ 12.12 (s, 1H), 8.65 (d,
345 *J* = 6.9 Hz, 2H), 8.22 (d, *J* = 6.9 Hz, 2H), 7.74 (d, *J* = 8.3 Hz, 2H), 7.68 (s, 1H), 7.57-7.55 (m,
346 4H), 7.48-7.32 (m 6H), 7.32 (d, *J* = 8.2 Hz, 1H), 6.21 (s, 2H), 2.27 (s, 3H). ¹³C NMR (75 MHz,
347 DMSO), 189.88, 171.71, 152.87, 151.87, 147.59, 146.99, 139.30, 130.21, 129.18, 129.00,
348 126.25, 125.70, 118.36, 114.77, 109.56, 108.65, 64.75, 25.06, HRMS for [M+H]⁺ calculated;
349 451.1652, found; 451.1658

350

351 **Planktonic growth phase antifungal activity assays.** Minimum inhibitory concentrations were
352 determined using CLSI guidelines (16, 20). All yeasts were cultured overnight in 3 mL YPD at
353 30°C, then washed twice in sterile PBS. Two-fold serial dilutions of each compound were
354 prepared in RPMI+MOPS pH 7 (Gibco RPMI 1640 with L-glutamine [11875-093] and 0.165M
355 MOPS), then 1 x 10³ cells were added per well. Plates were incubated at 37°C for 24 h (*C.*
356 *albicans* and *S. cerevisiae*) or 72 h (*C. neoformans*). For *A. fumigatus* and *F. oxysporum* wells
357 were inoculated with 1.25 x 10⁴ conidia. Plates were incubated at 37°C for 48 h for *A. fumigatus*
358 and 72 h for *F. oxysporum*.

359

360 **Biofilm phase antifungal activity assays.** These assays were performed as previously
361 described (17, 19). *C. albicans* and *C. auris*, overnight cultures were washed in sterile PBS and
362 adjusted to 1x10⁶ CFU/mL in RPMI+MOPS pH 7. 100μL cells were added to each well and

363 incubated at 37°C for 24 h. A two-fold dilution series of the compounds was prepared in RPMI +
364 MOPS with equal vehicle concentrations. Media was removed and biofilms were gently washed
365 with PBS, then 200µL of each drug dilution was added to wells and plates were incubated at
366 37°C for an additional 24 h. Media was removed and biofilms were gently washed with PBS,
367 then 100 µL of XTT solution (0.83 mg/mL XTT sodium salt [Sigma, Cat# X4626] + 32 µg/mL
368 PMS [Sigma, Cat# P9625] in PBS) was added to each well. Plates were incubated at 37°C for
369 30 min, then the absorbance was measured at 490 nm.

370
371 **Red blood cell lysis assay.** Hemolysis assays were performed with defibrinated sheep's blood
372 (Lampire, Cat# 7239001). Blood was washed three times with PBS then resuspended to ~50%
373 hematocrit in PBS. A two-fold dilution series of the compounds in 200µL PBS with equal DMSO
374 concentration across the series, then red blood cells were added with a final concentration of
375 2% hematocrit. Cells were incubated at RT for 2 h in a v-bottom microtiter plate, then plates
376 were spun down and supernatant was transferred to a flat bottom microtiter plate for
377 absorbance measurement at 570 nm. Compounds were tested in technical triplicate in at least
378 two independent assays performed on different days.

379
380 **Mammalian cell culture toxicity assay.** HepG2 cells (ATCC, #) were maintained and cultured
381 in HepG2 media (DMEM (Gibco, Cat#11965-092) with 5% FBS, 20 mM Glutamine, and
382 Penicillin/Streptomycin) at 37°C with 5% CO₂. Cells were seeded in 96-well plates at a density
383 of 1.25 x 10⁴ cells/well and incubated overnight at 37°C with 5% CO₂, then media was removed
384 and replaced with media containing a two-fold dilution series of compounds with equal DMSO
385 concentrations across all wells including no compound controls. Cells were incubated for an
386 additional 24 h. Supernatant was removed and used to quantify lactate dehydrogenase release
387 using the CyQuant LDH assay kit (Invitrogen, Cat#C20300) following the manufacturer's

388 directions. LDH signal was normalized to a max lysis control. The remaining cells were then
389 used to quantify cellular metabolism by XTT. Briefly, cells were washed, then 0.9 mg/mL XTT
390 (Sigma, CAT#X4626) + 320 µg/mL PMS (Phenothiazine methosulfate; Sigma, Cat# P9625) in
391 HepG2 media was added to each well. Plates were incubated at 37°C, with 5% CO₂ for 2 h,
392 then absorbance was measured at 490 nm.

393

394 **Rat model of *Candida albicans* vascular catheter infection.** *C. albicans* biofilm growth during
395 infection of implanted medical devices was measured using an external jugular-vein, rat-
396 catheter infection model (23). Briefly, a 1 x 10⁶ cells/ml inoculum for each strain or strain
397 combination was allowed to grow on an internal jugular catheter placed in a pathogen-free
398 female rat (16-week old, 400 g) for 24 h. After this period, the catheter volumes were removed
399 and the catheters were flushed with 0.9% NaCl. The biofilms were dislodged by sonication and
400 vortexing. Viable cell counts were determined by dilution plating. Three replicates were
401 performed for each strain.

402 Scanning electron microscopy of catheter biofilms. After a 24 h biofilm formation phase,
403 the devices were removed, sectioned to expose the intraluminal surface, and processed for
404 SEM imaging. Briefly, one milliliter fixative (4% formaldehyde and 1% glutaraldehyde in PBS)
405 was added to each catheter tube and tubes were fixed at 4 °C overnight. Catheters were then
406 washed with PBS prior to incubation in 1% OsO₄ for 30 min. Samples were then serially
407 dehydrated in ethanol (30–100%). Critical point drying was used to completely dehydrate the
408 samples prior to palladium–gold coating. Samples were imaged on a SEM LEO 1530, with
409 Adobe Photoshop 2022 (v. 23.2.2) used for image compilation.

410

411 **Porcine skin model of *Candida auris* colonization.** The collection of porcine skin samples
412 was conducted under protocols approved by the University of Wisconsin–Madison Institutional

413 Animal Care and Use Committee in accordance with published National Institutes of Health
414 (NIH) and United States Department of Agriculture (USDA) guidelines. Excised skin was
415 cleaned and shaved as described previously (24). Full-thickness samples were obtained by 12
416 mm punch and placed in 12-well plates containing 3 mL Dulbecco's Modified Eagle Medium
417 (DMEM) (Lonza, Walkersville, MD, USA) supplemented with 10% fetal bovine serum (FBS)
418 (Atlanta biologicals, Lawrenceville, GA, USA), penicillin (1,000 U/mL), and streptomycin (1
419 mg/mL) (Corning, Manassas, VA, USA) for 6 hours. Tissues were rinsed in DPBS and moved to
420 semi-solid media (6:4 ratio of 1% agarose (BIO-RAD, Hercules, CA, USA) in DPBS:DMEM with
421 10% FBS). Paraffin wax was applied around the edge of the skin and 10 μ L *C. auris* suspended
422 in synthetic sweat medium at 10^7 cells/mL was applied. Samples were incubated at 24 h and
423 compound A (8 μ g/mL or 16 μ g/mL) in synthetic sweat medium was applied. After 24 h a sterile
424 swab was used to remove compound from skin surface. Samples were vortexed in DPBS and
425 plated on YPD + chloramphenicol to assess viable burden.

426

427 **Acknowledgements**

428 This work was funded in part by NIH grants: R21AI164578 and R01AI161973 (DJK);
429 F32AI145160 (SRB), and R01AI073289 (DRA). Purchase of the NMR spectrometer used to
430 obtain results included in this publication was supported by the National Science Foundation
431 under the MRI award CHE-2117776. The authors thank Steven Riesinger and Tsvetelina
432 Lazarova (Med Chem Partners) for additional medicinal chemistry support of this project.

433

434 **References**

- 435 1. Wiederhold NP. 2022. Pharmacodynamics, mechanisms of action and resistance, and
436 spectrum of activity of new antifungal agents. *J Fungi (Basel)*. 8:857.
- 437 2. Perfect JR, Krysan DJ, Del Poeta M, Selmecki AM, Brown JCS, Cowen LE. 2022.
438 Editorial: Antifungal Pipeline: build it strong; build it better. *Front Cell Infect Microbiol*.

- 439 12:881272.
- 440 3. Taff HT, Mitchell KF, Edward JA, Andes DR. 2013. Mechanisms of *Candida* biofilm drug
441 resistance. *Future Microbiol.* 8:1325-1337.
- 442 4. Kean R, Ramage G. 2019. Combined antifungal resistance and biofilm tolerance: the
443 global threat of *Candida auris*. *mSphere.* 4:e00458-19.
- 444 5. Pappas PG, Kauffman CA, Andes DR, Clancy CJ, Marr KA, Ostrosky-Zeichner L, Reboli
445 AC, Schuster MG, Vazquez JA, Walsh TJ, Zaoutis TE, Sobel JD. 2016. Clinical practice
446 guideline for the management of candidiasis: 2016 update by the Infectious Diseases
447 Society of America. *Clin Infect Dis.* 62:e1-50.
- 448 6. Mermel LA, Allon M, Bouza E, Craven DE, Flynn P, O'Grady NP, Raad II, Rijnders BJ,
449 Sherertz RJ, Warren DK. 2009. Clinical practice guidelines for the diagnosis and
450 management of intravascular catheter-related infection: 2009 update the Infectious
451 Diseases Society of America. *Clin Infect Dis.* 49:1-45.
- 452 7. Horton MV, Nett JE. 2020. *Candida auris* infection and biofilm formation: going beyond
453 the surface. *Curr Clin Microbiol Rep.* 7:51-56.
- 454 8. Johnson CJ, Eix EF, Lam BC, Wartman KM, Meudt JJ, Shanmuganayagam D, Nett JE.
455 2021. Augmenting the activity of chlorhexidine for decolonization of *Candida auris* from
456 porcine skin. *J Fungi* 7:804.
- 457 9. Rybak JM, Cuomo CA, David Rogers P. 2022. The molecular and genetic basis of
458 antifungal resistance in the emerging fungal pathogen *Candida auris*. *Curr Opin*
459 *Microbiol.* 70:102208.
- 460 10. Jacobs SE, Jacobs JL, Dennis EK, Taimur S, Rana M, Patel D, Gitman M, Patel G,
461 Schaefer S, Iyer K, Moon J, Adams V, Lerner P, Walsh TJ, Zhu Y, Anower MR, Vaidya
462 MM, Chaturvedi S, Chaturvedi V. 2022. *Candida auris* pan-drug-resistant to four classes
463 of antifungal agents. *Antimicrob Agents Chemother.* 66:e0005322.
- 464 11. Chen SC, Biswas C, Bartley R, Widmer F, Pantarat N, Obando D, Djordjevic JT, Ellis

- 465 DH, Jolliffe KA, Sorrell TC. 2010. In vitro antifungal activities of
466 bis(alkylpyridinium)alkane compounds against pathogenic yeasts and molds. *Antimicrob*
467 *Agents Chemother.* 54:3233-40.
- 468 12. Shen M, Li PT, Wu YJ, Lin CH, Chai E, Chang TC, Chen CT. The antifungal activities
469 and biological consequences of BMVC-12C-P, a carbazole derivative against *Candida*
470 species. *Med Mycol.* 58:521-529.
- 471 13. Edlind MP, Smith LW, Edlind TD. 2005. Effects of cetylpyridinium chloride resistance
472 and treatment on fluconazole activity versus *Candida albicans*. *Antimicrob Agents*
473 *Chemother* 49:843-845.
- 474 14. Simm C, Weerasinghe H, Thomas DR, Harrison PF, Newton HJ, Beilharz TH, Traven A.
475 2022. Disruption of iron homeostasis and mitochondrial metabolism are promising
476 targets to inhibit *Candida auris*. *Microbiol Spectr.* 10:e0010022.
- 477 15. Obando D, Koda Y, Pantarat N, Lev S, Zuo X, Bijosono Oei J, Widmer F, Djordjevic JT,
478 Sorrell TC, Jolliffe KA. 2018. Synthesis and evaluation of a series of
479 bis(pentylpyridinium) compounds as antifungal agents. *ChemMedChem.* 13:1421-1436.
- 480 16. Beattie SR, Krysan DJ. 2021. A unique dual-readout high throughput screening assay to
481 identify antifungal compounds with *Aspergillus fumigatus*. *mSphere.* 6(4):e0053921.
- 482 17. Mao X, Auer DL, Buchalla W, Hiller KA, Maisch T, Hellwig E, Al-Ahmad A, Cieplik F.
483 2020. Cetylpyridinium chloride: mechanism of action, antimicrobial efficacy in biofilms,
484 and potential risks of resistance. *Antimicrob Agents Chemother.* 64:e00576-20.
- 485 18. White TC. 1997. Increased mRNA levels of *ERG16*, *CDR* and *MDR1* correlate with
486 increases in azole resistance in *Candida albicans* isolates from a patient infected with
487 human immunodeficiency virus. *Antimicrob Agents Chemother.* 41:1482-1487.
- 488 19. Ramage G, Vande Walle K, Wickes BL, López-Ribot JL. 2001. Standardized method for
489 in vitro antifungal susceptibility testing for *Candida albicans* biofilms. *Antimicrob Agents*
490 *Chemother.* 45:2475-2479.

- 491 20. Widerhold NP. 2021. Antifungal susceptibility testing: a primer for clinicians. Open
492 Forum Infect Dis. 8:ofab444.
- 493 21. Hoffman JJ, Arunga S, Mohamed Ahmed AHA, Hu VH, Burton MJ. 2022. Management
494 of filamentous fungal keratitis: a pragmatic approach. J Fungi (Basel). 8:1067.
- 495 22. Chandra J, Long L, Isham N, Mukherjee PK, DiSciullo G, Appelt K, Ghannoum MA.
496 2018. In vitro and in vivo activity of a novel catheter lock solution against bacterial and
497 fungal biofilms. Antimicrob Agents Chemother. 62:e00722-18.
- 498 23. Nett JE, Marchillo K, Andes DR. 2012. Modeling of fungal biofilms using a rat central
499 vein catheter. Methods Mol Biol. 845:547-556.
- 500 24. Johnson CJ, Cheong JZA, Shanmuganayagam D, Kalan LR, Nett JE. Modeling *Candida*
501 *auris* colonization on porcine skin ex-vivo. Methods Mol Biol. 2517:251-258.
- 502 25. Huang X, Hurabielle C, Drummond RA, Bouladoux N, Desai JV, Sim CK, Belkaid Y,
503 Lionakis MS, Segre JA. 2021. Murine model of colonization with fungal pathogen
504 *Candida auris* to explore skin tropism, host risk factors, and therapeutic strategies. ell
505 Host Microbe. 29:210-221.

506
507
508
509
510
511

512 **Figure Legends**

513 **Figure 1. Ketoalkylpyridinium compounds with aryl substitutions have tunable antifungal**
514 **activity. A.** The pharmacore and R₁ substitutions for compounds A, B and C with minimum
515 inhibitory concentrations (MIC; µg/mL) for *C. albicans* SC5314, *C. auris* 0381, and *A. fumigatus*
516 CEA10. **B.** Fractional inhibitory concentration indices (FICI) of B with clinical antifungals. FICIs

517 were calculated using the MIC ($\mu\text{g}/\text{mL}$) of each drug alone (MIC_A) and in combination (MIC_C)
518 based on at least two independent checkboard assays performed on separate days.
519 Interactions are defined as: $0.5 \geq \text{FICI} = \text{synergy}$; $0.5 < \text{FICI} < 2 = \text{additive}$; $2 < \text{FICI} < 4 =$
520 indifferent; $\text{FICI} \geq 4 = \text{antagonism}$.

521

522 **Figure 2. KAPs are active against fungal biofilms.** A. Metabolic activity of *A. fumigatus*
523 CEA10 biofilms (measured using resazurin) treated with increasing concentrations B or C for 24
524 hours. B. Propidium Iodide (PI) staining of *A. fumigatus* CEA10 hyphal cells treated with
525 $16\mu\text{g}/\text{mL}$ B for 24 hours. Images were acquired using the same exposure and magnification for
526 all samples. Representative images from two independent experiments. Metabolic activity of
527 established *C. albicans* SC5314 (**C**) or *C. auris* 0381 (**D**) biofilms treated with **A** or **C** for 24
528 hours. For all graphs, data represent mean and SEM of three biological replicates and are
529 normalized to untreated controls. IC_{50} curves and values were calculated using GraphPad Prism
530 9.

531

532 **Figure 3. KAPs are efficacious in a rat model of *C. albicans* infection of a vascular**
533 **catheter.** A. Colony forming units (CFU) of *C. albicans* from central venous catheters places in
534 rats and treated with vehicle or **A** ($8\mu\text{g}/\text{mL}$). Fungal burden data are shown as the mean and
535 SEM of log-transformed CFU values; $n=3$ rats per group. $**p<0.0001$ by unpaired t-test of log-
536 transformed values. B. Scanning electron micrographs of catheters treated with vehicle or 8
537 $\mu\text{g}/\text{mL}$ **A**. Scale bar = $10\mu\text{m}$.

538

539 **Figure 4. KAP A reduces *C. auris* colonization of skin in an ex vivo porcine model.** CFUs
540 of *C. auris* on porcine skin treated with vehicle or **A** ($8\mu\text{g}/\text{mL}$ or $16\mu\text{g}/\text{mL}$) for 24 h. Data

541 represent mean and SEM of log-transformed values; n=12 per group. **p<0.0001 by unpaired t-
542 test of log-transformed values.

543

544 **Figure S1. Chemical synthesis of compound A.** Reaction conditions: (a) PCl_5 (1.5 eq), 2 h,
545 reflux 150°(b) 30 min, 180°C, reflux (c) 2 h, 100°C acetonitrile reflux.

546

547 **Figure S2. Red blood cell and mammalian cell culture toxicity of KAP compounds. A.**

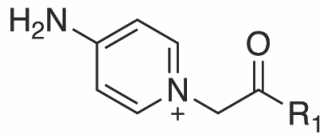
548 Hemolysis of commercial red blood cells (RBC) treated for 2 h with increasing concentrations of
549 KAPs normalized to max lysis by triton-x. Mean and SD of technical triplicates. Representative
550 data from three independent experiments performed on different days are shown. Toxicity
551 against HepG2 cells using LDH release (**B**) and XTT (**C**) assays. Cells were treated with the
552 indicated concentration series of **A** for 24 h. Mean and SD of technical triplicates. Data are
553 representative of two independent experiments performed on different days.

554

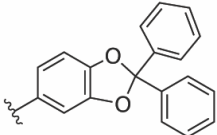
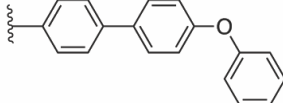
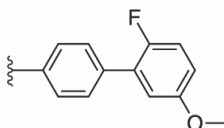
555

556

A



bioRxiv preprint doi: <https://doi.org/10.1101/2023.01.19.524833>; this version posted January 20, 2023. The copyright holder for this preprint (which was not certified by peer review) is the author/funder, who has granted bioRxiv a license to display the preprint in perpetuity. It is made available under aCC-BY-ND 4.0 International license.

Compound	<i>C. albicans</i> MIC	<i>C. auris</i> MIC	<i>A. fumigatus</i> MIC
A 	4	8	32
B 	8	16	8
C 	>128	>128	>128

B

Species	Clinical antifungal	B				FICI
		MIC _A	MIC _C	MIC _A	MIC _C	
<i>C. albicans</i>	Fluconazole	16	4	0.125	1	8.25
<i>C. albicans</i>	Amphotericin B	4	1	0.5	0.25	0.75
<i>A. fumigatus</i>	Voriconazole	16	2	0.25	0.125	0.625

Figure 2

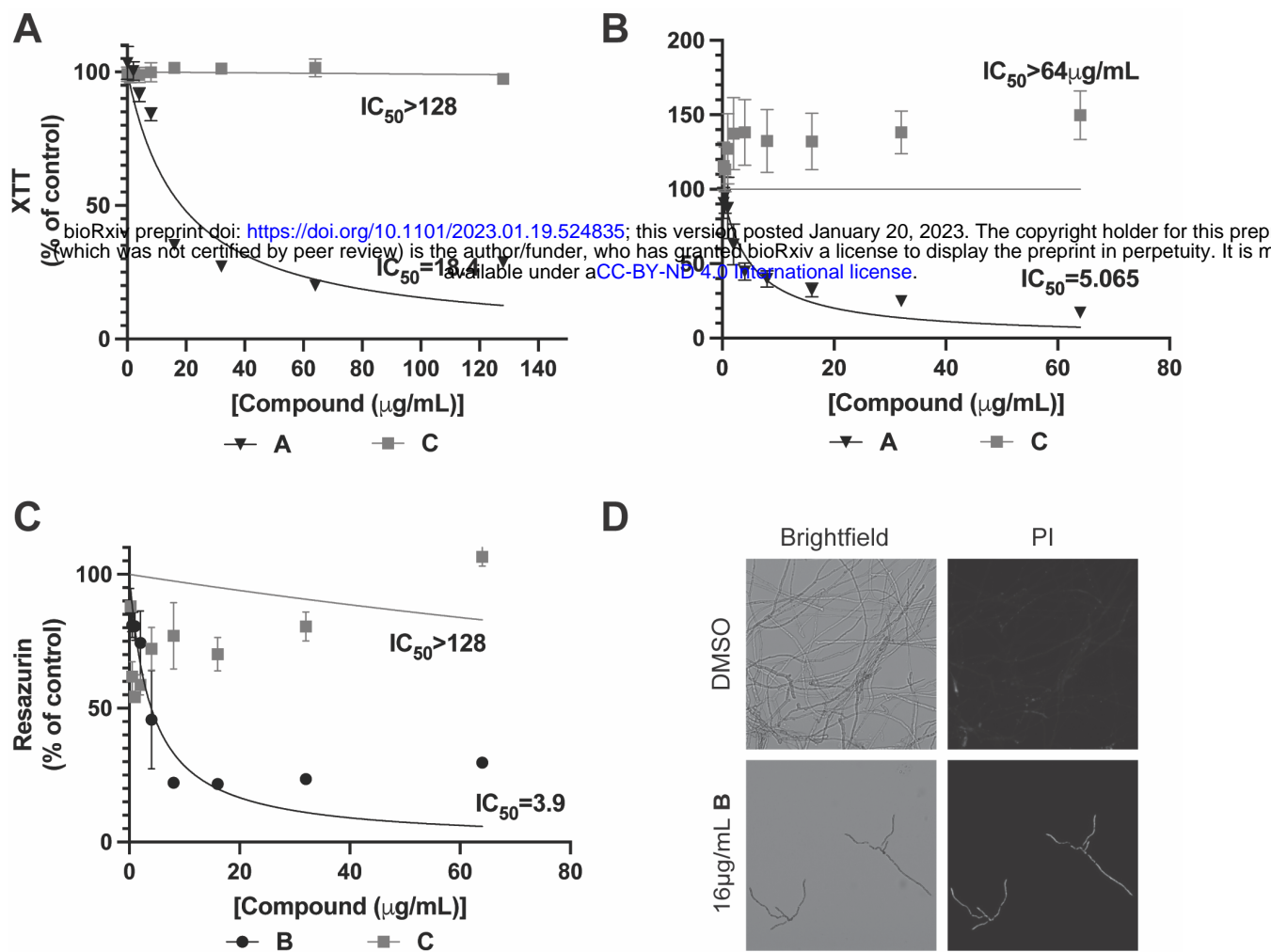


Figure 3

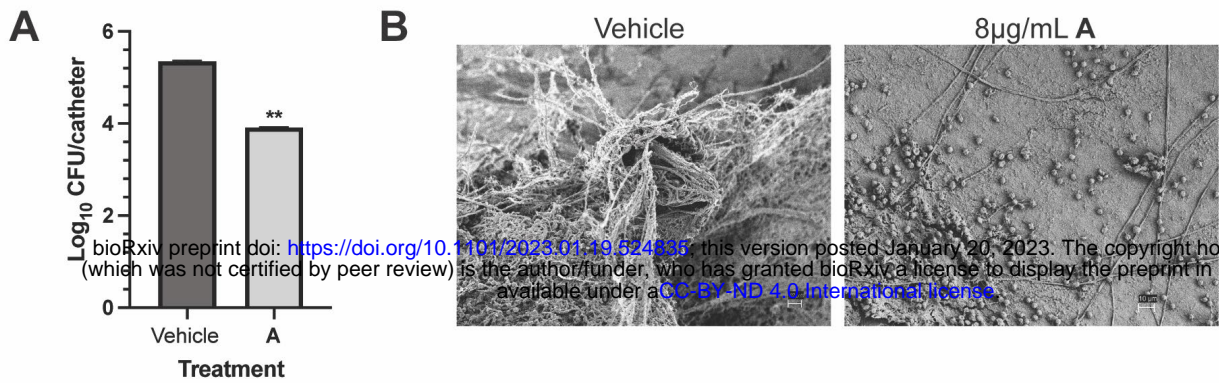
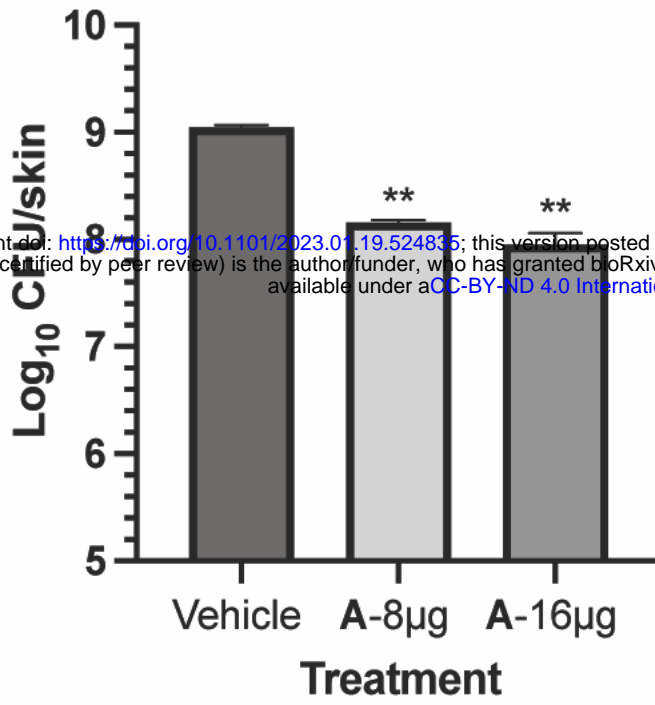


Figure 4



bioRxiv preprint doi: <https://doi.org/10.1101/2023.01.19.524835>; this version posted January 20, 2023. The copyright holder for this preprint (which was not certified by peer review) is the author/funder, who has granted bioRxiv a license to display the preprint in perpetuity. It is made available under aCC-BY-ND 4.0 International license.

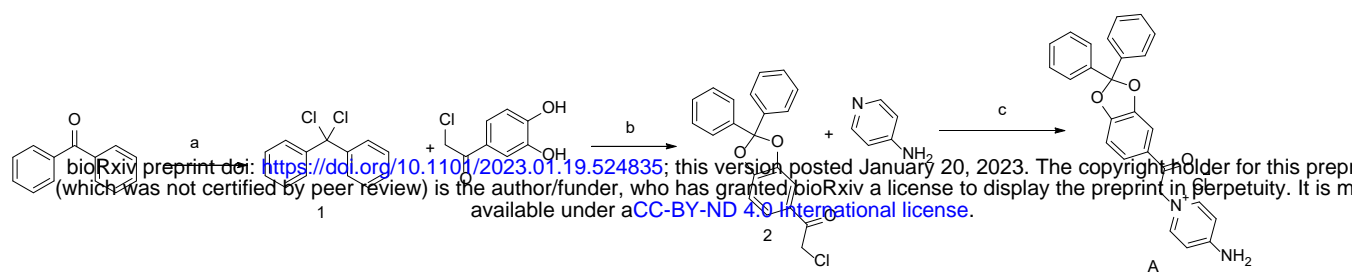
Table 1

Species	Strain	A MIC	B MIC
<i>A. fumigatus</i>	CEA10	32	8
	AF293	2	1
	SPF98	64	16
<i>C. albicans</i>	CFF S014	8	NT
	CFF S008	64	NT
	CFF S007	64	NT
	CFF S001	64	NT
	CFF S029	4	NT
	CFF S003	4	NT
	CFF S010	64	NT
	CFF S023	2-4	NT
<i>C. glabrata</i>	SC5314	4	8
	TWO #15	4	4
	TWO #17	4	4
<i>C. auris</i>	0381	8	16
	0390	2	4
<i>C. neoformans</i>	H99	4	2
	DUMC 118.00	4	2
	DUMC 122.01	4	4
<i>F. oxysporum</i>	DUMC Fo	16	16
<i>P. aeruginosa</i>	PAO1	64	32
<i>S. aureus</i>	Newman	32	16

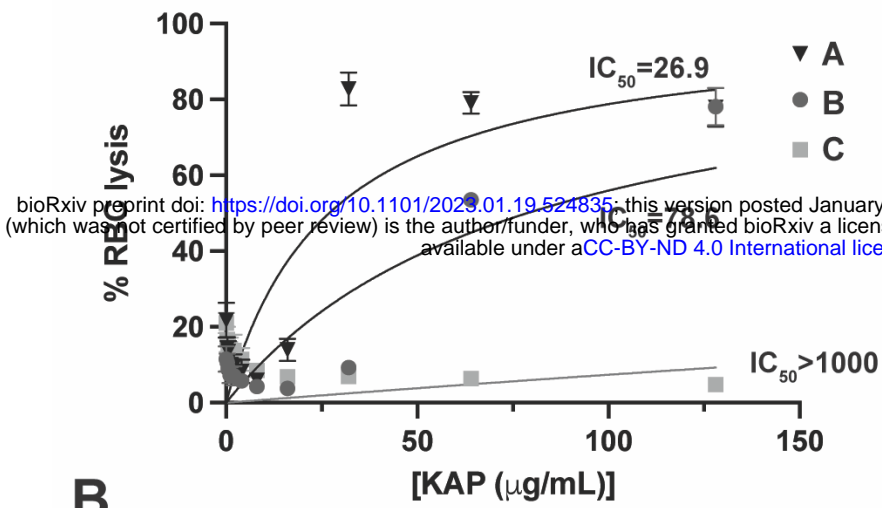
bioRxiv preprint doi: <https://doi.org/10.1101/2023.01.19.524835>; this version posted January 20, 2023. The copyright holder for this preprint (which was not certified by peer review) is the author/funder, who has granted bioRxiv a license to display the preprint in perpetuity. It is made available under aCC-BY-ND 4.0 International license.

Table 1. Minimum inhibitory concentration of KAP compounds against medically important fungi and bacteria. Minimum inhibitory concentrations (MIC; $\mu\text{g}/\text{mL}$) were measured using standard CLSI broth microdilution assays. Reported MICs are representative of at least two independent assays performed on different days. NT = not tested.

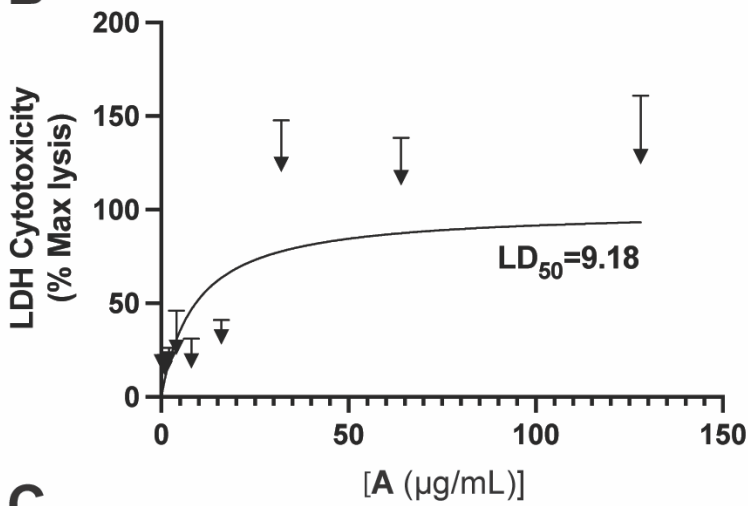
Figure S1



A



B



C

